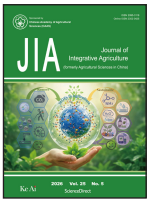
Journal of Integrative Agriculture 2026, 25(5): 2063–2076

Available online at ScienceDirect

Journal of Integrative Agriculture



RESEARCH ARTICLE

Residual nitrogen exhibits lower stability and greater influence on wheat yield formation compared to phosphorus and potassium in drylands of the Loess Plateau

Yufeng Wang[1], Zixuan Chang[1], Jiayu Wang[1], Tingliang Li[1, 2#], Zhiping Yang[1, 2#]

[1] *College of Resources and Environment, Shanxi Agricultural University, Taigu 030801, China*
[2] *Soil Health Laboratory in Shanxi Province, Taiyuan 030031, China*

Highlights

- NO_3-N and light fraction organic N (LFON) influenced wheat yield formation through regulation of spike number and kernels per spike.
- Prolonged N deficiency decreased both soil labile and recalcitrant N fractions.
- P and K deficiency predominantly affected labile fractions of soil P and K.
- Soil residual N pool demonstrated lower stability compared to P and K pools.

Abstract

Following the implementation of China's "Zero-Growth Action Plan on Fertilizers" in 2015, research has predominantly focused on replacing synthetic fertilizers with organic amendments to address over-fertilization concerns. However, insufficient attention has been given to the sustainable supply capacity of soil residual nutrients accumulated from previous over-fertilization. To investigate the transformation dynamics and supply capacity of residual nutrients during crop production, a six-year field experiment was conducted in the dryland wheat growing region of China's Loess Plateau. Five treatments were established: farmer's fertilization (FF), regulated fertilization (RF), regulated fertilization without N (RF-N), regulated fertilization without P (RF-P), and regulated fertilization without K (RF-K). The study examined wheat yield formation, variations and stability of soil N, P, and K fractions, and their correlations with yield. Results indicated that wheat yield sensitivity to nutrient deficiency followed the sequence N>P>K. During the six-year period, the average yield under RF-N decreased by 22.0% compared to RF, showing statistical significance (P<0.05). Mineral N, light fraction organic N (LFON), and heavy fraction organic N (HFON) in RF-N showed progressive decline relative to RF and initial 2018 levels. Dissolved organic N (DON) and easily oxidizable organic N (EON) in RF-N initially decreased but subsequently increased due to N fraction transformations. Under RF-P, H_2O-P, $NaHCO_3$-P, and NaOH-P levels decreased by 40.0, 51.5, and 10.3% respectively (P<0.05) compared to the RF treatment, while HCl-P, residual P, and total P (TP) remained stable. The absence of K application (RF-K) reduced water-soluble K (WSK) by 10.9% (P<0.05), whereas exchangeable K (EK), non-exchangeable K (NEK), mineral K (MK), and total K (TK) showed no significant changes compared to the RF treatment. These findings demonstrated that the soil nitrogen pool exhibits lower stability compared to phosphorus and potassium pools during continuous residual nutrient supply. Notably, NO_3-N and LFON significantly influenced spike number and kernels per spike, driving yield formation. This research advances our understanding of sustained residual nutrient supply capacity in soil and provides theoretical foundations for optimizing fertilization strategies in dryland agroecosystems.

Keywords: dryland wheat, yield formation, soil nutrient fractions, soil residual nutrient supply capacity, calcareous soil

Received 1 April 2025; Received in revised form 4 June 2025; Accepted 29 August 2025; Available online 26 September 2025
Yufeng Wang, E-mail: luckytll@yeah.net; #Correspondence Tingliang Li, E-mail: litingliang021@126.com; Zhiping Yang, E-mail: yzpsx0208@163.com

© 2026 CAAS. Publishing services by Elsevier B.V. on behalf of KeAi Communications Co. Ltd. This is an open access article under the CC BY-NC-ND license (http://creativecommons.org/licenses/by-nc-nd/4.0/). Peer review under responsibility of Editorial Board of *Journal of Integrative Agriculture*.
doi: 10.1016/j.jia.2025.09.029

1. Introduction

Chemical fertilizers, essential nutrients for crop growth, have significantly enhanced global agricultural productivity, contributing over 40% of yield increases. However, excessive and inappropriate application has resulted in substantial soil degradation, environmental pollution, and economic challenges (Jin *et al.* 2020; Ding *et al.* 2022; Yang W J *et al.* 2024). Addressing these concerns, Ministry of Agriculture and Rural Affairs of China launched the "*Action Plan for Zero Growth in Fertilizer Usage by 2020*" in 2015, initiating nationwide efforts to enhance fertilization practices through partial replacement of chemical fertilizers with organic alternatives and implementation of precision fertilization management. Despite these advances, research regarding the efficiency of residual soil nutrients from previous high fertilizer applications remains insufficient. Understanding the sustained supply capacity of soil nutrients during crop production provides crucial scientific insights for developing effective fertilization strategies and promoting sustainable, low-carbon agricultural practices.

Nitrogen fertilizer constitutes the primary nutrient input for crop production, and in China, excessive agricultural fertilizer usage primarily stems from nitrogen fertilizer overapplication. Recent studies demonstrate that substituting 30% of chemical fertilizers with organic alternatives can maintain high yields and fertilizer efficiency (Zhai *et al.* 2022; Wen *et al.* 2024; Mi *et al.* 2025; Zhang F *et al.* 2025). Nevertheless, historical chemical fertilizer overuse has resulted in substantial residual nitrate nitrogen accumulation in soils. In China's semi-humid agricultural regions, the average total nitrate accumulation at 4 m depth reached 453, 749, 1,191, 1,269, and 2,155 kg N ha^{-1} for wheat, maize, open-field vegetables, solar plastic-roofed greenhouse vegetables, and orchard fields, respectively (Zhou *et al.* 2016). Soil nitrogen transformation dynamics are manifested in the distribution of soil nitrogen fractions. Bremner (1965) classified soil organic nitrogen (SON) into acid-hydrolysable N (AHN) and non-hydrolysable N (NHN), with AHN further subdivided into amino acid N (AAN), acid-hydrolysable ammonium N (AHAN), amino sugar N (ASN), and hydrolysable unknown N (HUN). Studies indicate that AHAN serves as a temporary nitrogen pool, AAN functions as a transitional pool, while ASN and HUN are integrally connected to nitrogen stabilization during soil nitrogen pool transformations (Jiang *et al.* 2014; Wu *et al.* 2019; Yuan *et al.* 2024). Soil nitrogen predominantly exists within soil organic matter. Recent research has categorized soil organic nitrogen fractions into dissolved organic nitrogen (DON), easily oxidizable organic nitrogen (EON), particulate organic nitrogen (PON), light fraction organic nitrogen (LFON), and heavy fraction organic nitrogen (HFON), corresponding to soil organic carbon components (Zhong *et al.* 2015; Yuan *et al.* 2023; Yang C D *et al.* 2024). This classification system, featuring simplified determination methods, identifies DON, EON, PON, and LFON as labile organic nitrogen fractions, while HFON represents a stable organic nitrogen component (Muqaddas *et al.* 2019; Zuo *et al.* 2023; Wang M J *et al.* 2024). Previous studies have established that fertilizer application and agricultural management practices significantly affect soil labile organic nitrogen levels while minimally impacting stable organic nitrogen (Sequeira *et al.* 2011; Zhang *et al.* 2022; Zhao *et al.* 2025). However, research examining the dynamics of both labile and stable organic nitrogen during soil nitrogen depletion processes remains insufficient.

Phosphate (P) is readily immobilized through binding with calcium in calcareous soils or with iron and aluminum in acidic soils. The current utilization rate of phosphate fertilizer during the growing season typically ranges between 10 and 20% (Biassoni *et al.* 2023; Channab *et al.* 2024; Jadav *et al.* 2024). To enhance understanding of phosphorus transformation dynamics in soil, researchers have employed various methods to evaluate soil phosphorus fractions based on soil properties and research objectives (Cheng *et al.* 2024; Wu *et al.* 2024; Xue *et al.* 2025). The Hedley sequential phosphorus extraction method, originally developed by Hedley *et al.* (1982) and subsequently refined by Tiessen *et al.* (1984), represents an established analytical approach. This method sequentially extracts soil samples using deionized water, 0.5 mol L^{-1} $NaHCO_3$, 0.1 mol L^{-1} NaOH, and 1 mol L^{-1} HCl. Each extracted phosphorus fraction is analyzed separately to determine its organic (Po) and inorganic (Pi) phosphorus content. Remaining phosphorus after extraction is designated as residual phosphorus. Studies have shown that labile P (Soluble-Pi, $NaHCO_3$-Pi, and $NaHCO_3$-Po) and moderately labile P (NaOH-Pi, NaOH-Po, and HCl-Pi) exhibit varying degrees of plant absorption and utilization. The majority of soil phosphorus exists as non-labile phosphorus (Residual-P), bound within mineral structures and largely inaccessible to plants (Wan *et al.* 2022; Biassoni *et al.* 2023; Zhang L H *et al.* 2025). Consequently, agricultural research has primarily focused on investigating P activation and bioavailability in response to external inputs and management practices (Cao *et al.* 2022; Khan *et al.* 2023; Chen *et al.* 2025). However, research examining native soil P pool transformation dynamics and supply capacity under long-term crop cultivation remains limited.

The potassium (K) content in soil depends on soil-forming parent materials and climate conditions. In China, potassium levels demonstrate a decreasing gradient from north to south and west to east. Soils containing mica and feldspar minerals typically possess higher potassium reserves. Soil potassium exists in three forms: available potassium (water-soluble and exchangeable), slowly available potassium (non-exchangeable), and fixed potassium (mineral-bound). Field straw retention returns substantial potassium from plants to soil and reduces mineral nitrogen fertilizer losses through short-term nitrogen immobilization (Zhao *et al.* 2014). The combination of biochar with potassium fertilizers enhances potassium retention, while potassium-solubilizing microorganisms (such as *Bacillus megaterium*) facilitate mineral potassium weathering through microbial processes (Zhao *et al.* 2021; Xia *et al.* 2024). Nevertheless, research examining soil potassium supply potential in northwest China remains relatively scarce.

In summary, previous research has thoroughly investigated methods for improving N, P, and K fertilizer use efficiency during crop growth. However, limited attention has focused

on morphological transformation patterns and sustained supply capacity of residual soil nutrients (N, P, and K) in subsequent cropping cycles. Furthermore, the relationship between sustained availability of residual soil nutrients and crop yield development requires further elucidation. To address these research gaps, a six-year field experiment was implemented in the Loess Plateau dryland wheat growing region. The study objectives were to: 1) determine dryland wheat yield response to sustained residual nutrient supply; 2) elucidate transformation dynamics and utilization characteristics of residual soil N, P, and K during continuous nutrient supply; and 3) evaluate soil N, P, and K nutrient pool stability throughout the supply process. The research hypothesis proposed that residual nutrients (N, P, and K) in loess dryland wheat field soils could provide continuous supply. However, variations in nutrient forms result in differing N, P, and K reutilization efficiencies and nutrient pool stability, leading to distinct yield formation contributions. The residual N pool exhibits lower stability and greater influence on yield sustainability compared to P and K pools.

2. Materials and methods

2.1. Study area

The experimental site, situated at coordinates 36°22′N and 111°35′E with an elevation of 648 m, is located in Hongtong County, Linfen City, Shanxi Province, China. This region exemplifies a typical dryland winter wheat cultivation area on the Loess Plateau. The local climate exhibits characteristics of a temperate continental monsoon, with an annual average temperature of 12.3°C. The frost-free period extends approximately 210 days annually, and the average annual sunshine duration is 2,079 h. The site soil is categorized as a calcic cinnamon soil according to the Chinese Soil Genetic Classification (CSGC), and as a calcareous silt loam under the USDA texture classification system.

Initial soil nutrient analysis conducted in 2018 at a depth of 0–20 cm revealed the following properties: organic matter (OM) of 11.98 g kg^{-1}, total nitrogen (TN) of 0.68 g kg^{-1}, nitrate nitrogen (NN) of 28.5 mg kg^{-1}, ammonium nitrogen (AN) of 2.8 mg kg^{-1}, available phosphorus (AP) of 8.7 mg kg^{-1}, available potassium (AK) of 170.8 mg kg^{-1}, and a pH level of 8.0. Throughout the experimental period from 2018 to 2024, the average annual precipitation measured 486 mm, with over 60% of rainfall occurring during the summer fallow period from June to September (Fig. 1).

2.2. Experimental design and management

Five experimental treatments were established to evaluate the residual soil nutrient supply capacity in dryland wheat cultivation on the Loess Plateau: (1) farmer's fertilization (FF), applying fertilizers at local farmers' average application rates; (2) regulated fertilization (RF), formulated with fertilizer quantities calculated to achieve designated yield targets while considering inherent soil nutrient supply capacity (Li *et al.* 2019); (3) regulated fertilization without N (RF-N); (4) Regulated fertilization without P (RF-P); and (5) regulated fertilization without K (RF-K). The experiment utilized a completely randomized block design with four replicates, each plot measuring 140 m^2 (25 m×5.6 m). Table 1 details the annual fertilizer application rates for each treatment throughout the experiment. The applied fertilizers consisted of urea (46.0% N), superphosphate (12% P_2O_5), and potassium sulfate (60% K_2O), all incorporated into the soil before winter wheat sowing.

Winter wheat cultivation during the experimental period employed a ridge-furrow sowing method. Ridges were covered with a plastic film of 0.008 mm thickness, while furrows remained uncovered and contained two rows of wheat, spaced 20 cm apart. The ridge dimensions measured 35 cm in width and 10 cm in height, with furrows of 30 cm width (Fig. 2). The seeding rate was maintained at 150 kg ha^{-1}. Planting occurred between September 30 and October 9, with annual harvesting from June 5 to June 10. The summer fallow period extended from mid-June to late September. Crops relied solely on natural precipitation, without supplemental irrigation. All straw from the experimental field was returned to the soil.

2.3. Sample collection and analysis

Wheat yield and yield components At physiological maturity, three 1-m row samples were collected from each experimental plot to evaluate yield components, including spike number, grains per spike, 1,000-grain weight, and harvest index. The entire plot was harvested using a small plot combine harvester, and grain yield was determined after threshing and drying to constant moisture content (<12.5%).

Soil nutrient fractions Soil samples were collected from a depth of 0–20 cm prior to winter wheat sowing in 2018, as well

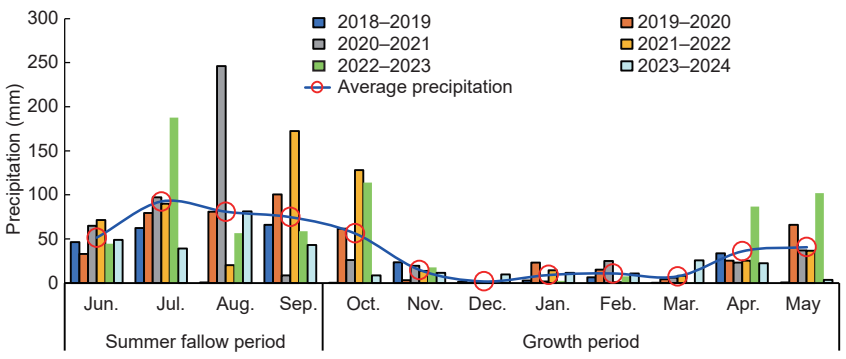


Fig. 1 Monthly precipitation at the experimental site during the growing and fallow periods between 2018 and 2024.

Table 1 Annual fertilizer application rates (kg ha^{-1}) for each treatment during the experimental period

Year	Treatment[1)]	N	P_2O_5	K_2O
2018–2019	FF	150	60	0
	RF	104	41	0
	RF-N	0	41	0
	RF-P	104	0	0
	RF-K	104	41	0
2019–2020	FF	150	60	0
	RF	86	51	30
	RF-N	0	51	30
	RF-P	86	0	30
	RF-K	86	51	0
2020–2021	FF	150	60	0
	RF	114	49	30
	RF-N	0	49	30
	RF-P	114	0	30
	RF-K	114	49	0
2021–2022	FF	150	60	0
	RF	76	43	30
	RF-N	0	43	30
	RF-P	76	0	30
	RF-K	76	43	0
2022–2023	FF	150	60	38
	RF	90	51	30
	RF-N	0	51	30
	RF-P	90	0	30
	RF-K	90	51	0
2023–2024	FF	103	126	60
	RF	163	63	30
	RF-N	0	63	30
	RF-P	163	0	30
	RF-K	163	63	0
2018–2024	FF	853	363	68
	RF	633	298	150
	RF-N	0	298	150
	RF-P	633	0	150
	RF-K	633	298	0

[1)] FF, farmer's fertilization; RF, regulated fertilization; RF-N, regulated fertilization without N; RF-P, regulated fertilization without P; RF-K, regulated fertilization without K.

as following harvests in 2021 and 2024, to analyze the fractions of soil nitrogen (N), phosphorus (P), and potassium (K).

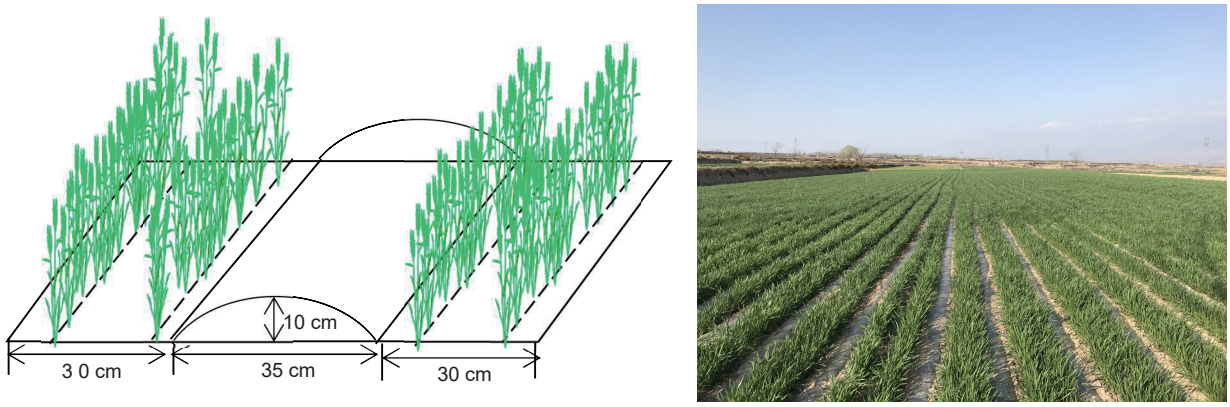
The soil N factions analyzed comprised mineral nitrogen (NO_3-N and NH_4-N), DON, EON, LFON and HFON. Mineral nitrogen (NO_3-N and NH_4-N) was extracted by shaking the soil sample with 1 mol L^{-1} KCl (soil:liquid=1:10) for 30 min, followed by quantification using a continuous flow analyzer (AA3, SEAL, Germany). The DON extraction involved shaking the sample with deionized water (soil:solution=1:20) for 30 min and filtering through 0.45-μm membranes. EON was oxidized by shaking the sample with 333 mmol L^{-1} $KMnO_4$ (soil:solution=1:25) for 1 h. The LFON and HFON were separated through density fractionation with a 1.7 g cm^{-3} NaI solution (Zhong *et al.* 2015; Yuan *et al.* 2023). The concentrations of DON, EON, LFON and HFON were determined using a CHNS-O analyzer (EMA 502, VELP, Italy).

The soil P fractions determination process involved weighing 0.5 g of soil sample and sequential extraction with deionized water, 0.5 mol L^{-1} $NaHCO_3$, 0.1 mol L^{-1} NaOH and 1 mol L^{-1} HCl by shaking for 16 h. The contents of H_2O-P, $NaHCO_3$-P, NaOH-P, and HCl-P were then determined. The residual P was determined through digestion with H_2SO_4 and 30% H_2O_2. Total P (TP) determination involved digestion with $HClO_4$ and H_2SO_4 (Cross and Schlesinger 1995; Biassoni *et al.* 2023; Zhang *et al.* 2023).

The soil K fractions analyzed included water-soluble K (WSK), exchangeable K (EK), non-exchangeable K (NEK) and mineral K (MK). WSK extraction involved shaking the sample with deionized water (soil:solution=1:10) for 30 min. EK was extracted by shaking the sample with 1 mol L^{-1} NH_4OAc (soil:solution=1:10) for 1 h and calculated as the difference between NH_4OAc-extracted K and WSK. For NEK determination, 5 g of soil was boiled with 50 mL of 1 mol L^{-1} HNO_3 in a 250 mL glass beaker (covered with a watch glass) for 10 min, followed by filtration. NEK was calculated by subtracting NH_4OAc-extracted K from HNO_3-extracted K. MK was determined by subtracting HNO_3-extracted K from total K (TK), with TK measured using the NaOH melting method (Wang *et al.* 2010; Zhang *et al.* 2020). All K fractions were quantified using a flame photometer (FP6410, JINGKE, China).

2.4. Statistical analysis

Data analysis was conducted using IBM SPSS 27.0 and Origin 2025. Differences among fertilization treatments (T)



Schematic diagram

Photo of the experimental field

Fig. 2 Schematic diagram and photo of the ridge-furrow sowing method.

and experimental years (Y) were evaluated through two-way analysis of variance (ANOVA; P<0.05), followed by the least significant difference (LSD) test. The relationships between soil N, P, and K fractions and winter wheat yield were analyzed using Pearson correlation coefficients and the Mantel test, implemented with the "psych" package in R. Structural equation modeling (SEM) was employed using AMOS software to examine the effects of N, P, and K fractions on winter wheat yield components.

3. Results

3.1. Response of wheat yield to fertilization

Dryland wheat grain yield showed significant responses to soil nutrient supply (Fig. 3-A). Six years of continuous experimentation demonstrated that grain yield sensitivity to soil nutrient deficiency followed the order: N>P>K, with statistically significant differences (P<0.05). The six-year average grain yield without N application (RF-N) decreased significantly by 25.8 and 22.0% compared to the FF and RF treatments, respectively (P<0.05). The harvest index (HI) showed no significant differences between RF-N and RF treatments during 2018–2022. However, HI under RF-N was significantly lower than other treatments in 2022–2023, but significantly higher in 2023–2024. Despite these fluctuations, the overall six-year mean HI remained statistically similar among RF, RF-N, RF-P, and RF-K treatments, averaging 43.1% (Fig. 3-B).

Analysis of yield components revealed that six years of N, P, or K deficiency significantly reduced spike number. Specifically, N and P deficiency decreased kernels per spike, while K deficiency reduced the 1,000-grain weight (Fig. 3-C–

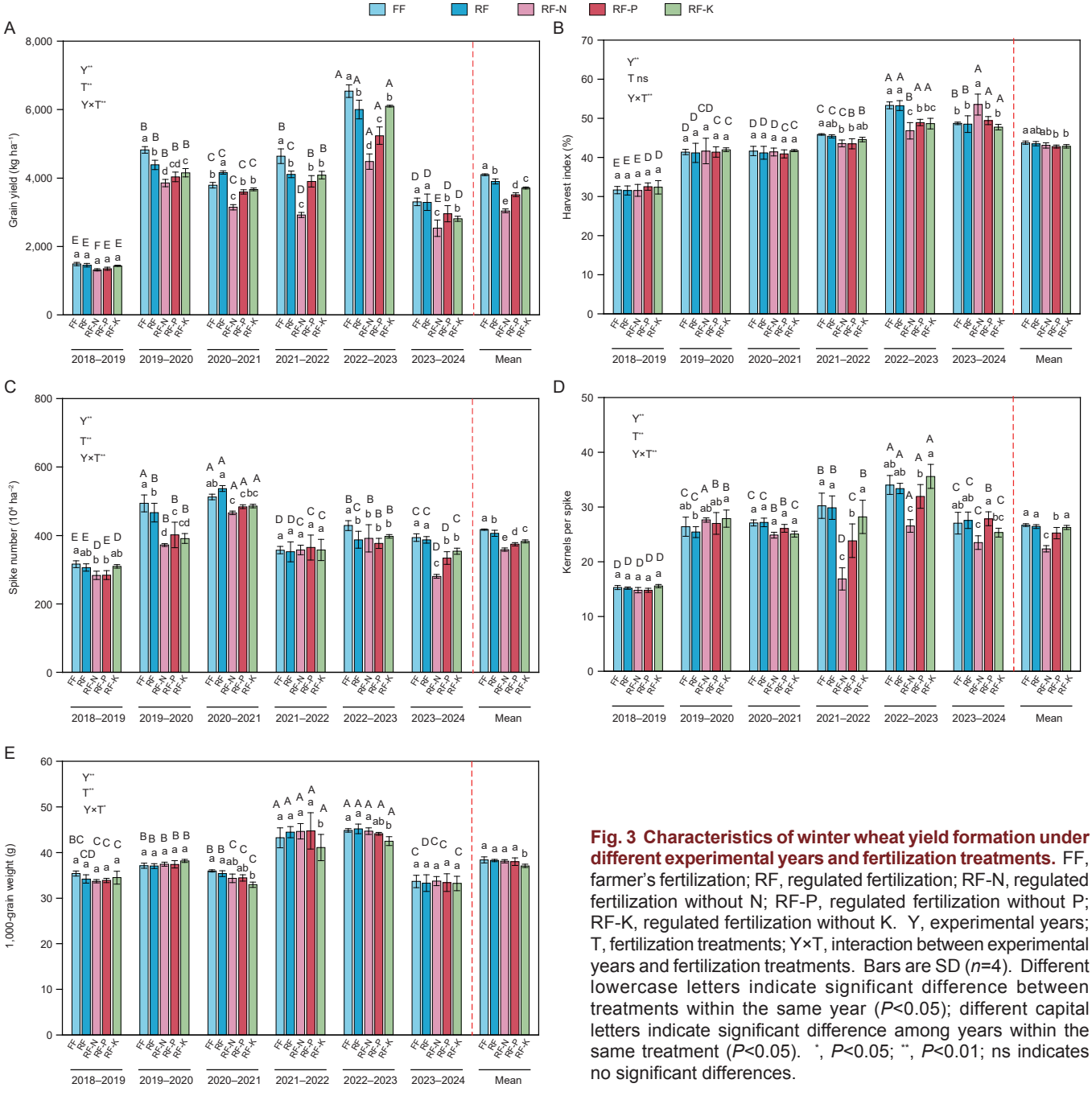


Fig. 3 Characteristics of winter wheat yield formation under different experimental years and fertilization treatments. FF, farmer's fertilization; RF, regulated fertilization; RF-N, regulated fertilization without N; RF-P, regulated fertilization without P; RF-K, regulated fertilization without K. Y, experimental years; T, fertilization treatments; Y×T, interaction between experimental years and fertilization treatments. Bars are SD (n=4). Different lowercase letters indicate significant difference between treatments within the same year (P<0.05); different capital letters indicate significant difference among years within the same treatment (P<0.05). *, P<0.05; **, P<0.01; ns indicates no significant differences.

E). These results indicate that soil nutrient stress primarily limits dryland wheat yield formation through reduced spike number and kernels per spike, with N deficiency exhibiting stronger effects than P or K deficiency. Furthermore, significant inter-annual variations (P<0.05) were observed across all measured parameters: spike number, kernels per spike, 1,000-grain weight, harvest index, and grain yield.

3.2. Dynamics of soil nitrogen fractions

From 2018 to 2024, mineral nitrogen content in the 0–20 cm soil layer showed a marked decline across all treatments, mainly due to decreasing NO_3-N levels. The RF-N treatment exhibited significantly lower NH_4-N and NO_3-N contents compared to other treatments (Fig. 4-A). DON contents under all N application treatments exceeded initial 2018 levels. However, the RF-N treatment showed significantly lower DON than the RF treatment. Specifically, DON content under RF-N treatment decreased by 41.3% during the first three years (P<0.05), followed by a 64.0% increase in the subsequent three years (P<0.05) (Fig. 4-B). The EON content in RF-N treatment decreased by 18.1% (2021) and 12.4% (2024) compared to RF treatment (P<0.05; Fig. 4-C). Three years of N deficiency significantly reduced topsoil LFON content, while HFON remained stable. After six years of N deficiency, both LFON and HFON contents decreased significantly in the RF-N treatment, leading to an 8.3% reduction in total soil organic nitrogen compared to 2018 pre-sowing levels (Fig. 4-D).

3.3. Dynamics of soil phosphorus fractions

Continuous P deficiency during wheat cultivation affected various soil P fractions differently. Compared to RF treatment, H_2O-P levels in the RF-P treatment decreased significantly by 21.4 and 40.0% after three and six consecutive years, respectively (P<0.05; Fig. 5-A). Similarly, $NaHCO_3$-P in RF-P treatment showed significant reductions of 28.2 and 51.5% after three and six years of P deficiency (P<0.05). Notably, six years of N deficiency resulted in increased $NaHCO_3$-P content (Fig. 5-B). Additionally, six years of P deficiency caused a 10.3% reduction in NaOH-P content compared to the RF treatment (P<0.05; Fig. 5-C). However, six consecutive years of deficiencies in N, P, and K did not significantly affect the contents of HCl-P, Residual-P, and TP (Fig. 5-D–F). These results demonstrate that H_2O-P and $NaHCO_3$-P represent the labile P fractions readily available to dryland wheat. NaOH-Pi functions as a buffer reservoir for soil P supply, while HCl-P and Residual-P maintain relative stability within the soil system with minimal transformation and plant availability.

3.4. Dynamics of soil potassium fractions

During the first three years of wheat cultivation, soil K fractions showed no significant differences across fertilization treatments, except for higher WSK and EK levels in RF-N and RF-P treatments compared to the RF-K treatment (P<0.05). After six years, the WSK content in the RF-K treatment was significantly lower than in the RF treatment. Moreover, the WSK level differences between RF-N, RF-P treatments and the RF-K treatment increased significantly (Fig. 6-A). EK content showed no significant differences between RF-K and RF treatments (Fig. 6-B). Six years of continuous differential fertilization demonstrated no significant effect on soil NEK, MK, and TK contents (Fig. 6-C–E).

3.5. Relationship between dryland wheat yield and soil nutrient fractions

Correlation heatmap analysis of dryland wheat yield and soil N, P, and K fractions (0–20 cm depth) at harvest in 2024 demonstrated significant positive correlations among LFON, HFON, EON, NH_4-N, and NO_3-N, with the strongest correlation coefficient (0.9070) between LFON and NO_3-N. Furthermore, significant positive correlations were observed between H_2O-P and $NaHCO_3$-P, $NaHCO_3$-P and NaOH-P, as well as between WSK and EK. Dryland wheat yield exhibited positive correlations with NH_4-N, NO_3-N, EON, and LFON, with LFON showing the strongest correlation (Fig. 7). SEM revealed relationships between soil N, P, and K fractions and dryland wheat yield components. Detailed analyses indicated that N fractions, represented by NO_3-N and LFON, demonstrated significant positive effects on spike number (r=0.911, P<0.01) and kernels per spike (r=0.783, P<0.01). P fractions, represented by H_2O-P and $NaHCO_3$-P, significantly positively influenced spike number (r=0.550, P<0.01). The spike number exhibited an extremely significant positive impact on wheat yield (Fig. 8).

4. Discussion

4.1. Effects of different fertilization practices on winter wheat yield in drylands

During the experimental period, substantial interannual variations in grain yield (ranging from 1,407 to 5,672 kg ha^{-1}) were observed across different precipitation years, with minimum and maximum yields recorded in 2018–2019 and 2022–2023, respectively (Figs. 1 and 3-A). These findings indicate that adequate soil moisture optimizes the synergistic relationship between winter wheat growth and soil nutrient supply, thereby enhancing yield potential. The experiments revealed differential sensitivity of grain yield to soil nutrient stress among fertilization treatments, following the order: N>P>K (Fig. 3-A). This pattern can be attributed to two interrelated mechanisms. First, the requirement for N during the growth and yield formation of winter wheat exceeds that for P and K. As documented by Cai *et al.* (2022), N accumulation in aboveground biomass exceeded that of P and K, with grain nitrogen content being higher (22.0 g kg^{-1}) than that of P (3.13 g kg^{-1}) and K (4.10 g kg^{-1}) under different mulching practices. Second, this phenomenon correlates with the content of soil available nutrients. In Northwest China, under diverse vegetation and climatic conditions, the content of soil available K significantly exceeds that of available P and available N (Shao *et al.* 2022).

In this study, the HI of winter wheat varied across different precipitation years. However, the six-year average HI showed no significant differences among RF, RF-N, RF-P, and RF-K (Fig. 3-B). This observation aligns with the study by Dai *et al.* (2016), who determined that crop HI is primarily

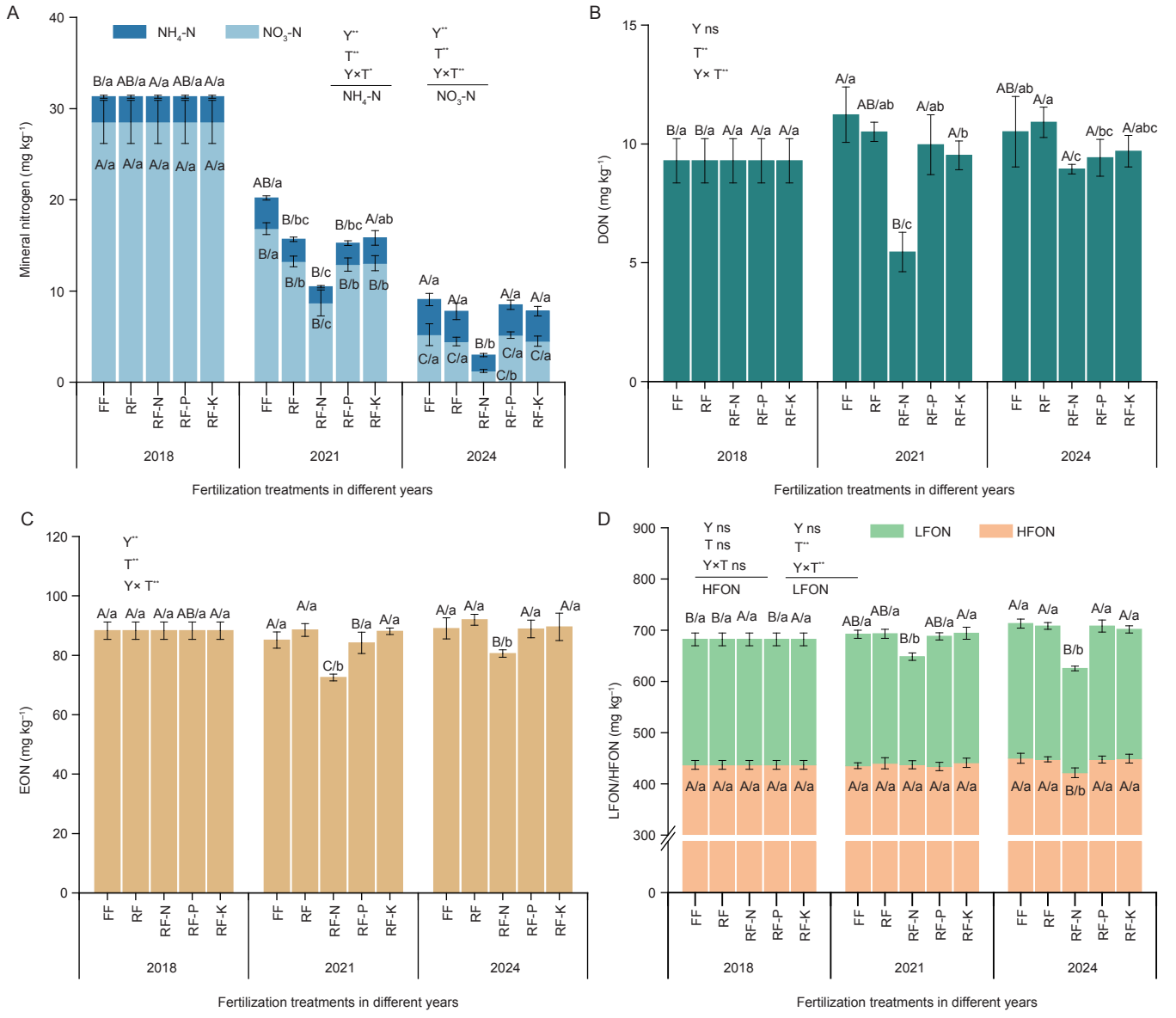


Fig. 4 Changes in soil nitrogen fractions under different experimental years and fertilization treatments. FF, farmer's fertilization; RF, regulated fertilization; RF-N, regulated fertilization without N; RF-P, regulated fertilization without P; RF-K, regulated fertilization without K. DON, dissolved organic nitrogen; EON, easily oxidizable organic nitrogen; LFON, light fraction organic nitrogen; HFON, heavy fraction organic nitrogen. Y, experimental years; T, fertilization treatments; Y×T, interaction between experimental years and fertilization treatments. Bars are SD (n=4). Different lowercase letters indicate significant difference (P<0.05) between treatments within the same year; different capital letters indicate significant difference (P<0.05) among years within the same treatment. *, P<0.05; **, P<0.01; ns indicates no significant differences.

governed by genetic variation within cereal classes and broad environmental variation across climate regions. Spike number was the primary factor influencing yield formation of winter wheat in drylands, followed by kernel number per spike (Dou *et al.* 2024). Consequently, N, P, and K stress affected the yield formation of dryland wheat by influencing population construction (spike number) and spikelet differentiation (kernel number per spike) (Figs. 3-C and D and 8). Conversely, 1,000-grain weight remained a relatively stable component, with its contribution to yield being substantially lower than that of spike number and kernel number per spike (Cai *et al.* 2022; Yang *et al.* 2022).

4.2. Effects of different fertilization practices on soil N supply capacity

The average content of TN in the arable layer soil of the Loess Plateau region is approximately 0.81 g kg^{-1} (Liu *et al.* 2013). Mineral nitrogen, the primary form absorbed and utilized by plants, comprises about 2% of the TN. The dominant fraction of TN is organic nitrogen, which undergoes microbial mineralization and serves as an essential potential N supply for crops (Zhang *et al.* 2024). During the six-year experimental period (2018–2024), all treatments demonstrated a decreasing trend in mineral nitrogen (Fig. 4-A), attributable to both plant assimilation and N leaching caused by precipitation. The treatments without

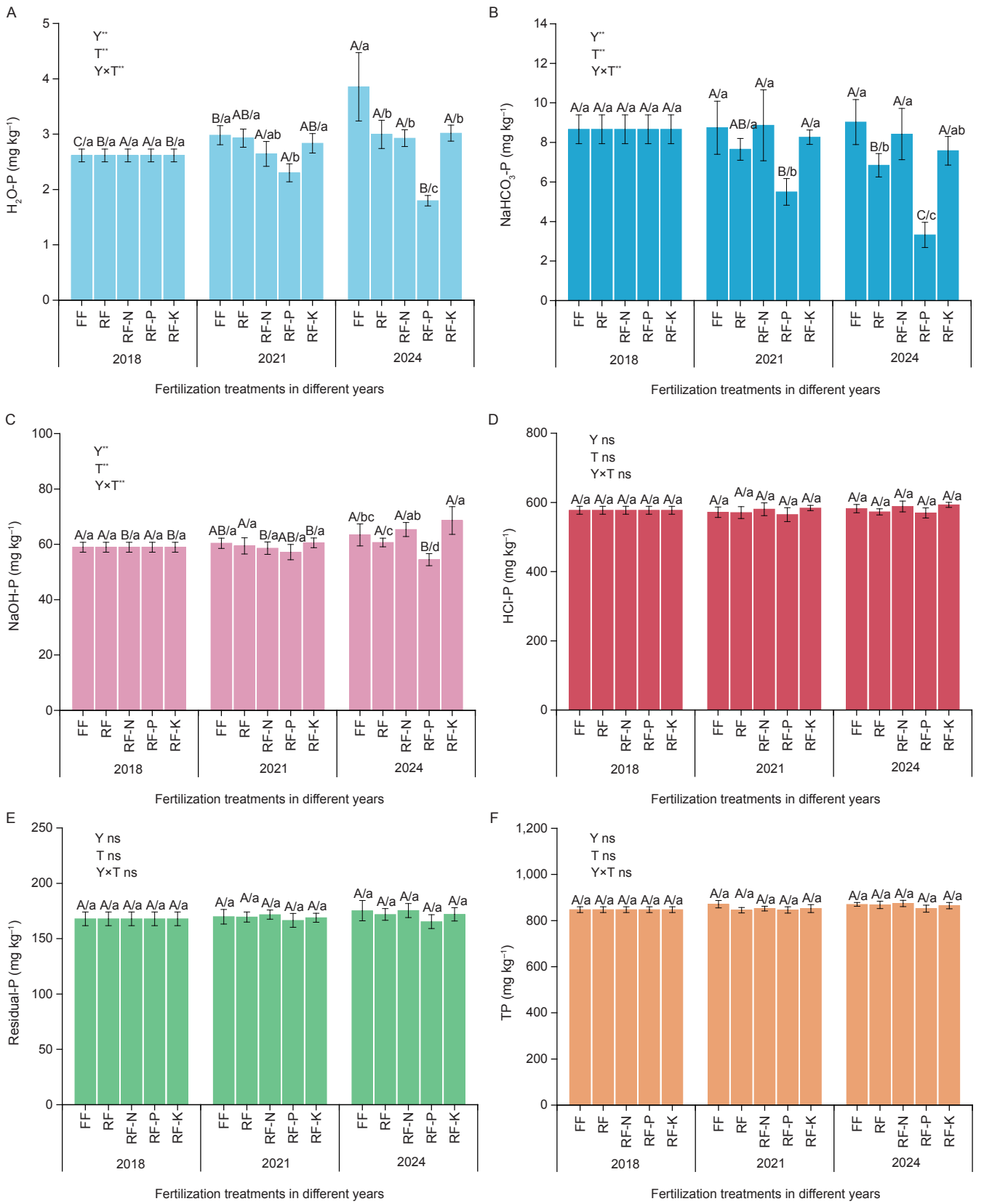


Fig. 5 Changes in soil phosphorus fraction under different experimental years and fertilization treatments. FF, farmer's fertilization; RF, regulated fertilization; RF-N, regulated fertilization without N; RF-P, regulated fertilization without P; RF-K, regulated fertilization without K. TP, total phosphorus. Y, experimental years; T, fertilization treatments; Y×T, interaction between experimental years and fertilization treatments. Bars are SD (n=4). Different lowercase letters indicate significant difference (P<0.05) between treatments within the same year; different capital letters indicate significant difference (P<0.05) among years within the same treatment. *, P<0.05; **, P<0.01; ns indicates no significant differences.

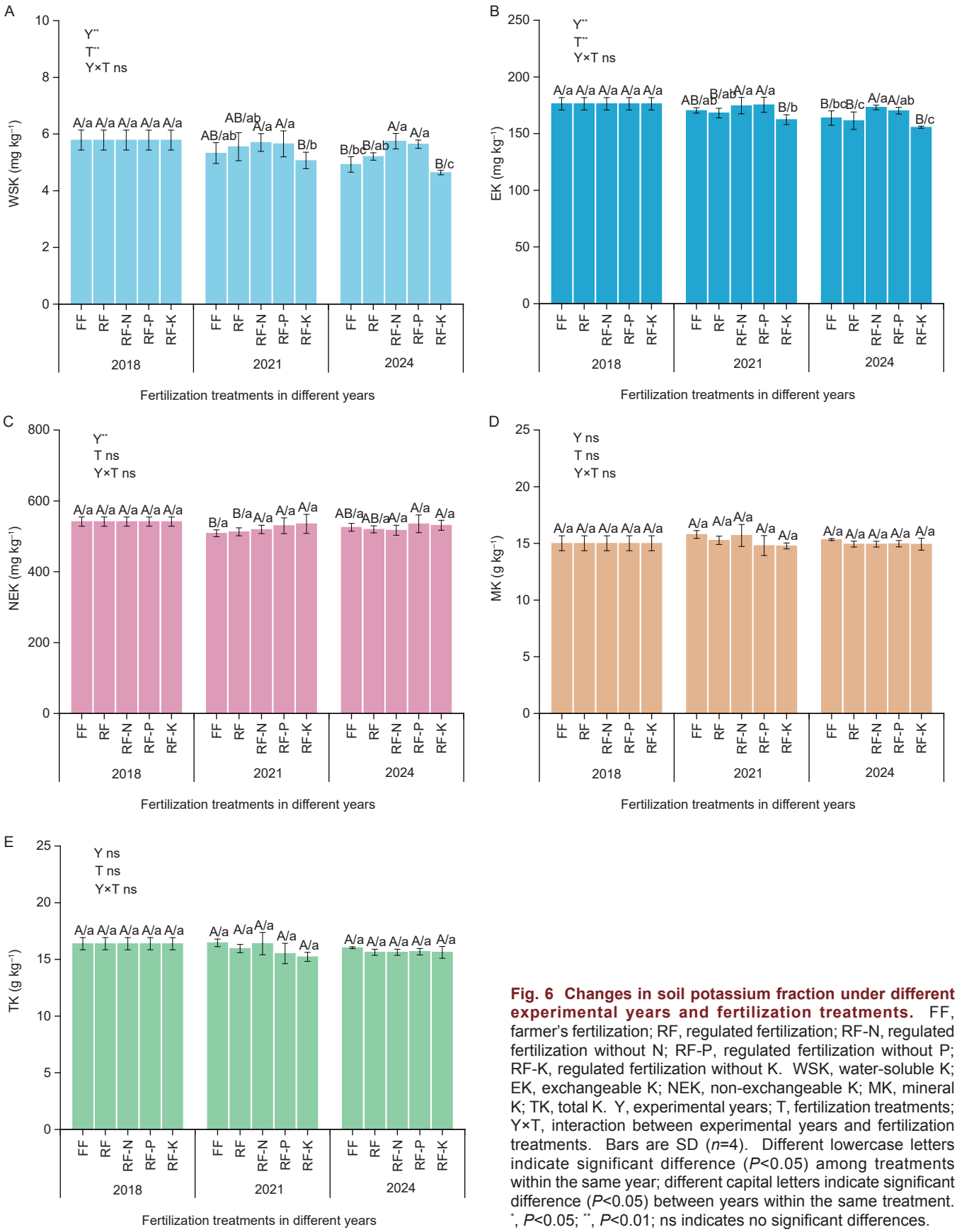


Fig. 6 Changes in soil potassium fraction under different experimental years and fertilization treatments. FF, farmer's fertilization; RF, regulated fertilization; RF-N, regulated fertilization without N; RF-P, regulated fertilization without P; RF-K, regulated fertilization without K. WSK, water-soluble K; EK, exchangeable K; NEK, non-exchangeable K; MK, mineral K; TK, total K. Y, experimental years; T, fertilization treatments; Y×T, interaction between experimental years and fertilization treatments. Bars are SD (n=4). Different lowercase letters indicate significant difference (P<0.05) among treatments within the same year; different capital letters indicate significant difference (P<0.05) between years within the same treatment. *, P<0.05; **, P<0.01; ns indicates no significant differences.

phosphorus (RF-P) and without potassium (RF-K) did not significantly affect the levels of different N fractions compared to the RF treatment. However, the treatment without nitrogen (RF-N) significantly reduced the contents of NH_4-N, NO_3-N, DON, EON, LFON and HFON (Fig. 4-B–D).

Soil DON and EON are considered crucial N sources

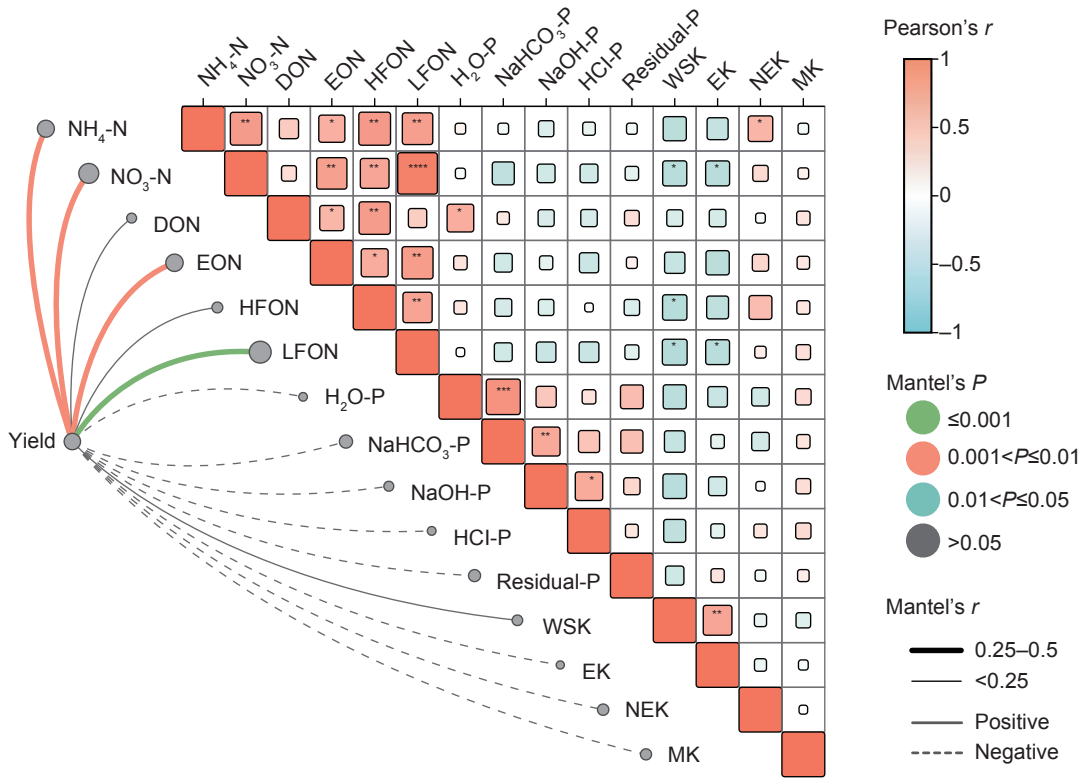


Fig. 7 Associations between dryland wheat yield and soil N, P and K fractions with the Mantel test. DON, dissolved organic nitrogen; EON, easily oxidizable organic nitrogen; LFON, light fraction organic nitrogen; HFON, heavy fraction organic nitrogen. WSK, water-soluble K; EK, exchangeable K; NEK, non-exchangeable K; MK, mineral K. The color of the color column represents the Pearson correlation coefficient between the indicators. The closer the blue color is, the stronger the negative correlation is, and the closer the red color is, the stronger the positive correlation is. *, P<0.05, **, P<0.01, ***, P<0.001, ****, P<0.0001.

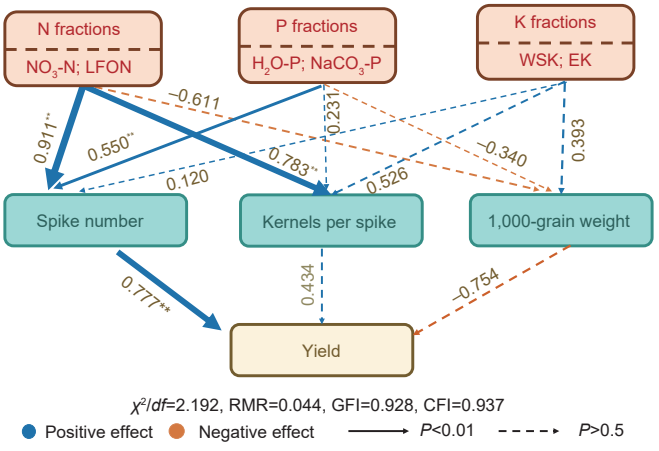


Fig. 8 Structural equation modelling describing the effects of soil N, P and K fractions on yield components of dryland wheat. LFON, light fraction organic nitrogen; WSK, water-soluble K; EK, exchangeable K. Arrow width corresponds to relationship strength. Numbers adjacent to arrows represent standardized path coefficients (**, P<0.01).

for plants and microbes and serve a central role in soil N turnover (Ros *et al.* 2010; Quan *et al.* 2018). Under RF-N treatment, the contents of DON and EON exhibited an initial decline followed by recovery during the 6-year experimental period, indicating their function as buffering pools during organic-to-inorganic nitrogen conversion. In contrast, LFON decreased by 16.9% (41.3 mg kg^{-1}) over the study period, establishing it as the primary reservoir for this conversion (Fig. 4-D). NH_4-N, NO_3-N, EON, and LFON significantly influenced dryland wheat yield (Fig. 7). Furthermore, NO_3-N and LFON contributed significantly to the formation of spike number and kernels per spike (Fig. 8). Previous studies have shown that LFON pools primarily comprise degraded plant material, microbial tissues, and substances not associated with mineral soil particles. These fractions demonstrate high responsiveness to agricultural management practices. Consequently, LFON can function as early indicators of management intervention impacts (Zhong *et al.* 2015; Chen *et al.* 2018; Wang *et al.* 2022).

The carbon-to-nitrogen (C/N) ratio of exogenous organic matter represents a primary limiting factor affecting its decomposition and transformation rates in soil. Research indicates that when the C:N ratio exceeds 25:1, microorganisms require additional soil N to facilitate organic matter degradation. In this study, under N-deficient conditions, the decomposition and mineralization of soil organic matter (organic nitrogen) accelerated unexpectedly. This acceleration was attributed to the inherently lower C:N ratio of the SOM itself. Without exogenous N inputs, plants extract N from existing soil organic matter (Wang *et al.* 2025). N deficiency triggers a “cry-for-help” mechanism, promoting symbiotic fungal interactions to enhance plant

nitrogen acquisition and mitigate N deficiency stress. Soil fungi enhance plant N uptake through hyphal network expansion, lateral root growth stimulation, and N transport activity regulation (Chan *et al.* 2025). Under N-deficient conditions, crop root length and root-to-shoot ratio increase (Lopez *et al.* 2023). Moreover, adequate P and K supply promotes plant N uptake by increasing leaf and root N-metabolizing enzyme activities, thereby improving N utilization efficiency (Liu *et al.* 2024). Zeng *et al.* (2023) demonstrated that N deficiency accelerated soil organic carbon decomposition, particularly recalcitrant carbon, in temperate degraded grasslands by influencing soil pH and microbial metabolism.

4.3. Effects of different fertilization practices on soil P supply capacity

In natural ecosystems, phosphorus serves as a critical limiting nutrient, released gradually through parent material weathering or internal recycling among nutrient pools (Brödlin *et al.* 2019; Gao *et al.* 2021). Root-mediated rhizosphere acidification enhances P mobilization by facilitating the dissolution of mineral-bound phosphate forms, particularly Ca-associated P (Hinsinger *et al.* 2003; Li *et al.* 2024). Furthermore, the metabolic activities of soil microbial communities, especially arbuscular mycorrhizal fungi (AMF), play a crucial role in activating soil phosphorus (Huo *et al.* 2022). In the present study, six years without P application (RF-P) significantly decreased the contents of H_2O-P, $NaHCO_3$-P, and NaOH-P in the soil. However, it showed no significant effect on the contents of HCl-P, Residual-P, and TP (Fig. 5). These findings suggest that plant roots in calcareous soils primarily utilize surface-adsorbed labile P, followed by Fe/Al-bound fractions, while demonstrating limited capacity to assimilate Ca/Mg-bound P and mineral-bound P. Moreover, H_2O-P and $NaHCO_3$-P contents exhibited significant positive correlations with spike number of dryland wheat (Fig. 8). A 26-year phosphorus addition and depletion experiment conducted by Liu *et al.* (2019) in the Huang-Huai-Hai Plain of China similarly demonstrated that phosphorus depletion reduced Olson-P content but did not significantly affect hydroxyapatite [$Ca_5(PO_4)_3OH$)] levels compared to the initial soil. However, phosphorus depletion increased Fe-P content, contrasting with our results. This disparity may reflect different temporal dynamics of phosphorus transformations. Specifically, NaOH-extractable phosphorus (Fe/Al-P) functions as a dynamic soil phosphorus buffer pool, undergoing consumption-replenishment cycles at various stages of phosphorus depletion. This phenomenon may not be fully evident in our shorter-term experiment.

In China's Loess Plateau, Khan *et al.* (2023) found that 25 years of continuous NPK fertilization (with P applied at 82.2 kg ha^{-1} yr^{-1}) resulted in a cumulative residual soil P pool (calculated as total P input minus crop P uptake) of 893 kg P ha^{-1}. Furthermore, the NPK treatment significantly elevated the contents of labile, moderately labile, and stable soil P fractions relative to the NK treatment. Zhu *et al.* (2018) reported that soil legacy P, which accumulated through historical inputs, served as an important potential secondary P source that could substitute (at least in part) for manufactured fertilizers. In our study, 21.1 t ha^{-1} of wheat was produced over six consecutive years under phosphorus-deficient conditions (Fig. 3-A), with no significant impact on the primary phosphorus fractions in the soil or on the stability of the soil phosphorus cycling system. These findings highlight the importance of activating soil legacy phosphorus for sustaining agricultural production. Additionally, seasonal dry-wet cycling in the study region serves as a critical driver for soil phosphorus activation and translocation (Brödlin *et al.* 2019).

4.4. Effects of different fertilization practices on soil K supply capacity

The parent materials derived in China's Loess Plateau contain abundant potassium-bearing minerals such as K-feldspar and micaceous minerals (He *et al.* 2015). Soil TK content typically ranges from 1 to 3%, substantially exceeding that of soil TN and TP. Soil K exists predominantly as NEK and MK, while WSK and EK constitute only 1–2% of the TK (Babar *et al.* 2024). Crop growth and physiological processes demonstrate high sensitivity to potassium availability in the soil; soil K deficiency or insufficient K supply can impede crop growth and reduce yield (Li *et al.* 2021; Wang C W *et al.* 2024). In this study, six years without K application (RF-K) resulted in a significant 10.9% decrease in topsoil WSK content compared to the RF treatment (P<0.05), while EK, NEK, MK, and TK levels remained statistically unchanged (Fig. 6). K deficiency correlated with substantial yield reduction in dryland winter wheat (Fig. 3-A).

Liu *et al.* (2025) determined that the critical thresholds of soil available K (WSK+EK) for preventing crop yield reduction were 159 mg kg^{-1} (wheat), 149 mg kg^{-1} (maize), and 94 mg kg^{-1} (rice), based on analysis of thirty-three Chinese long-term experiments. Similarly, Yang W J *et al.* (2024) analyzed data from 60 field experimental sites in China's drylands and established that the critical nutrient value for available potassium in topsoil for dryland wheat production was 150 mg kg^{-1}. The present study's results indicated that dryland wheat yields decreased significantly when soil available potassium (WSK+EK) content fell below 160 mg kg^{-1} (Fig. 6-A and B). Annual straw return in the experimental field contributes to replenishing soil available potassium. Research by Chuan *et al.* (2013) demonstrated that wheat straw returns approximately 80% of the K absorbed by aboveground biomass. At the yield levels observed in this experiment, six years without K application (RF-K) significantly reduced the WSK content, likely due to inherently low WSK levels. However, no significant changes in EK content were observed.

This research comprises a multi-year experiment conducted at a single site in the dryland wheat region of the Loess Plateau. The results revealed significant interannual variations in winter wheat yield, yield components, and soil nutrient fractions. Water availability significantly influences nutrient absorption, utilization and yield formation in dryland wheat systems. The variations in precipitation across different years (Fig. 1) likely explain the annual differences observed in measured indicators. Notably, despite varying

precipitation conditions throughout the experimental period, the response of wheat yield formation to fertilization practices demonstrated consistent patterns. Although this research was limited to a single site in the dryland wheat area of the Loess Plateau, it potentially reflects yield formation and nutrient absorption patterns across different precipitation regions under similar soil conditions, offering valuable theoretical insights for scientific nutrient management in dryland wheat production systems.

5. Conclusion

This six-year field experiment conducted in wheat fields of the Loess Plateau demonstrated that winter wheat yield sensitivity to soil nutrient stress followed the order: N>P>K. Extended periods without N, P, or K fertilization led to significant yield reductions. Under continuous utilization of residual soil nutrients, both labile N fractions (NH_4-N, NO_3-N, DON, EON, LFON) and recalcitrant N fractions (HFON) decreased to varying degrees under N deficiency. Phosphorus deficiency reduced labile P pools (H_2O-P, $NaHCO_3$-P, NaOH-P), while stable P fractions (HCl-P, residual P) remained constant. Potassium deficiency decreased WSK content but did not significantly affect the contents of EK, NEK and MK. Wheat yield demonstrated the strongest positive correlation with LFON and NO_3-N contents, which critically influence spike number and kernels per spike, thereby determining yield formation. Scientific fertilization strategies for sustainable and environmentally conscious agricultural production must consider both the inherent nutrient supply capacity and soil nutrient pool stability. Future research should evaluate the economic and environmental implications of soil P and K activation technologies as potential alternatives to chemical fertilizer inputs for P and K in calcareous soils in Northwest China.

Acknowledgements

This work was supported by the National Key Research and Development Program of China (2023YFD1900402 and 2021YFD1900700), the National Natural Science Foundation of China (42377356), and the special fund for Science and Technology Innovation Teams of Shanxi Province, China (202304051001042).

Declaration of competing interest

The authors declare that they have no conflicts of interest.

Declaration of generative AI and AI-assisted technologies in the writing process

The authors declare that they did not use AI in the preparation and writing of this manuscript.

References

Babar S, Baloch A, Qasim M, Wang J Y, Wang X L, Li Y X, Khalid S, Jiang C C. 2024. Unearthing the soil-bacteria nexus to enhance potassium bioavailability for global sustainable agriculture: A mechanistic preview. *Microbiological Research*, **288**, 127885.

Biassoni M M, Vivas H, Guti´errez-Boem F H, Salvagiotti F. 2023. Changes in soil phosphorus (P) fractions and P bioavailability after 10 years of continuous P fertilization. *Soil and Tillage Research*, **232**, 10577.

Bremner J M. 1965. Total nitrogen. In: *Methods of Soil Analysis.* Part 2. Chemical and Microbiological Properties. American Society of Agronomy, USA. pp.1149–1178.

Brödlin D, Kaiser K, Kessler A, Hagedorn F. 2019. Drying and rewetting foster phosphorus depletion of forest soils. *Soil Biology and Biochemistry*, **128**, 22–34.

Cao N, Zhi M L, Zhao W Q, Pang J Y, Hu W, Zhou Z G, Meng Y L. 2022. Straw retention combined with phosphorus fertilizer promotes soil phosphorus availability by enhancing soil P-related enzymes and the abundance of *phoC* and *phoD* genes. *Soil & Tillage Research*, **220**, 105390.

Chai Y W, Chai Q, Han F X, Li Y W, Ma J T, Li R, Cheng H B, Chang L, Chai S X. 2022. Increasing yields while reducing soil nutrient accumulation by straw strip mulching in the dryland wheat (*Triticum aestivum* L.) cropping system of Northwest China. *Agriculture, Ecosystems and Environment*, **326**, 107797.

Chan H L, Lam S K, Chen D L, Tang C X, Chen Q L, Roessner U, Hu H W. 2025. Nitrogen deficiency drives fungal compositional shifts without functional changes in wheat rhizosphere. *Rhizosphere*, **33**, 101030.

Channab B E, Tayi F, Aqlil M, Akil A, Essamlali Y, Chakir A, Zahouily M. 2024. Graphene oxide, starch, and kraft lignin bio-nanocomposite controlled-release phosphorus fertilizer: Effect on P management and maize growth. *International Journal of Biological Macromolecules*, **282**, 137190.

Chen X D, Wang Y, Guo B, Liu J L, Qiu G Y, Yakov K, Li H. 2025. Long-term green manuring increases phosphorus availability in soil by modifying microbial functional genes and enzyme activities. *Applied Soil Ecology*, **213**, 106284.

Chen Y M, Xu X, Jiao X G, Sui Y Y, Liu X B, Zhang J Y, Zhou K, Zhang J M. 2018. Responses of labile organic nitrogen fractions and enzyme activities in eroded mollisols after 8-year manure amendment. *Scientific Reports*, **8**, 14179.

Cheng L, Cui H, Ou Y, Wang L X, Bao M W. 2024. Redistribution of phosphorus fraction driven by organic carbon and microbial community during composting. *Journal of Environmental Management*, **370**, 123003.

Chuan L M, He P, Jin J Y, Li S T, Grant C, Xu X P, Qiu S J, Zhao S C, Zhou W. 2013. Estimating nutrient uptake requirements for wheat in China. *Field Crops Research*, **146**, 96–104.

Cross A F, Schlesinger W H. 1995. A literature review and evaluation of the Hedley fractionation: Applications to the biogeochemical cycle of soil phosphorus in natural ecosystems. *Geoderma*, **64**, 197–214.

Dai J, Bean B, Brown B, Bruening W, Edwards J, Flowers M, Karow R, Lee C, Morgan G, Ottman M, Ransom J, Wiersma J. 2016. Harvest index and straw yield of five classes of wheat. *Biomass and Bioenergy*, **85**, 223–227.

Ding J P, Li J H, Liu J H, Zhang W F, Jia X P. 2022. ICT-based agricultural advisory services and nitrogen management practices: A case study of wheat production in China. *Journal of Integrative Agriculture*, **21**, 1799–1811.

Dou Y X, Zhao H B, Yang H M, Wang T, Liu G F, Wang Z H, Malhi S. 2024. The first factor affecting dryland winter wheat grain yield under various mulching measures: Spike number. *Journal of Integrative Agriculture*, **23**, 836–848.

Gao X L, Li X G, Zhao L, Kuzyakov Y. 2021. Shrubs magnify soil phosphorus depletion in Tibetan meadows: Conclusions from C: N:P stoichiometry and deep soil profiles. *Science of the Total Environment*, **785**, 147320.

He P, Yang L P, Xu X P, Zhao S C, Chen F, Li S T, Tu S H, Jin J Y, Johnston A M. 2015. Temporal and spatial variation of soil available potassium in China (1990–2012). *Field Crops Research*, **173**, 49–56.

Hedley M J, Stewart J W B, Chauhan B. 1982. Changes in inorganic and organic soil phosphorus fractions induced by cultivation practices and by laboratory incubations. *Soil Science Society of America Journal*, **46**, 970–976.

Hinsinger P, Plassard C, Tang C, Jaillard B. 2003. Origins of root-mediated pH changes in the rhizosphere and their responses to environmental constraints: A review. *Plant and Soil*, **248**, 43–59.

Huo W G, Chai X F, Wang X H, William D B, Kafle A, Gu F. 2022. Indigenous arbuscular mycorrhizal fungi play a role in phosphorus depletion in organic manure amended high fertility soil. *Journal of Integrative Agriculture*, **21**, 3051–3066.

Jadav K, Durgam M, Perli M, Mailapalli D R. 2024. Phosphorus transport modeling in soils treated with nano-phosphorus fertilizers. *Plant Nano Biology*, **10**, 100112.

Jiang H M, Li S S, Zhang J F, Yang J C, Li L L, Zhang S Q, Guo J M, Liu L, Xie Y Q, Wang F Y. 2014. Transformation of external chemical nitrogen in soil organic nitrogen fractions and their relationship. *Journal of Plant Nutrition and Fertilizer*, **20**, 1421–1430. (in Chinese)

Jin Z X, Wang J F, Chen J G, Zhang R X, Li Y, Lu Y T, He K K. 2020. Identifying the sources of nitrate in a small watershed using $\delta^{15}N$-$\delta^{18}O$ isotopes of nitrate in the Kelan Reservoir, Guangxi, China. *Agriculture, Ecosystems and Environment*, **297**, 106936.

Khan A, Yang X Y, Sun B H, Zhang S L, He B H. 2023. Responses of crop and soil phosphorus fractions to long-term fertilization regimes in a loess soil in northwest China. *Agronomy*, **13**, 3072.

Li C, Ma X, Wang Y, Sun Q, Chen M S, Zhang C S, Ding S M, Dai Z H. 2024. Root-mediated acidification, phosphatase activity and the phosphorus-cycling microbial community enhance phosphorus mobilization in the rhizosphere of wetland plants. *Water Research*, **255**, 121548.

Li T L, Xie Y H, Gao Z Q, Hong J P, Li L, Meng H S, Ma H M, Jia J X. 2019.Year-round film mulching system with monitored fertilization management improve grain yield and water and nitrogen use efficiencies of winter wheat in the dryland of the Loess Plateau, China. *Environmental Science and Pollution Research*, **26**, 9524–9535.

Li Z L, Zhang W T, Qiu L X, Pan T L, Zheng W K, Kong B, Wang H L, Li C L, Liu Z G, Zhang M. 2021. Physiological-biochemical responses of wheat to blending controlled-release potassium chloride and soluble potassium chloride. *Soil & Tillage Research*, **212**, 105058.

Liu J, Sui P, Cade-Menun B J, Hu Y F, Yang J J, Huang S M, Ma Y B. 2019. Molecular-level understanding of phosphorus transformation with long-term phosphorus addition and depletion in an alkaline soil. *Geoderma*, **353**, 116–124.

Liu Y, Gao J P, Zhong M, Chen L Q, Zhang W Z. 2024. Effects of phosphorus and potassium supply on photosynthetic nitrogen metabolism, nitrogen absorption, and nitrogen utilization of hydroponic rice. *Agronomy*, **14**, 1726.

Liu Z J, Yuan X H, Zhang Z X, Yang X Y, Ai C, Wang Z H, Fan Q L, Xu X P. 2025. Revisiting potassium-induced impacts on crop production and soil fertility based on thirty-three Chinese long-term experiments. *Field Crops Research*, **322**, 109732.

Liu Z P, Shao M A, Wang Y Q. 2013. Spatial patterns of soil total nitrogen and soil total phosphorus across the entire Loess Plateau region of China. *Geoderma*, **197–198**, 67–78.

Lopez G, Ahmadi S H, Amelung W, Athmann M, Ewert F, Gaiser T, Gocke M I, Kautz T, Postma J, Rachmilevitch S, Schaaf G, Schnepf A, Stoschus A, Watt M, Yu P, Seidel S J. 2023. Nutrient deficiency effects on root architecture and root-to-shoot ratio in arable crops. *Frontier in Plant Science*, **13**, 1067498.

Mi X T, Xie W Y, Fan L, Zhang T L, Liu Y R, He G. 2025. Paired nitrogen management for improving wheat yields while minimizing nitrogen losses. *Journal of Integrative Agriculture*, **24**, 3626–3640.

Muqaddas B, Lewis T, Esfandbod M, Chen C R. 2019. Responses of labile soil organic carbon and nitrogen pools to long-term prescribed burning regimes in a wet sclerophyll forest of southeast Queensland, Australia. *Science of the Total Environment*, **647**, 110–120.

Quan Z, Huang B, Lu C Y, Shi Y, Chen X, Zhou J B, Fang Y T. 2018. Formation of extractable organic nitrogen in an agricultural soil: A ^{15}N labeling study. *Soil Biology and Biochemistry*, **118**, 161–165.

Ros G H, Hoffland E, Temminghoff E J M. 2010. Dynamics of dissolved and extractable organic nitrogen upon soil amendment with crop residues. *Soil Biology and Biochemistry*, **42**, 2094–2101.

Shao W Y, Wang Q Z, Guan Q Y, Luo H P, Ma Y R, Zhang J. 2022. Distribution of soil available nutrients and their response to environmental factors based on path analysis model in arid and semi-arid area of northwest China. *Science of the Total Environment*, **827**, 154254.

Sequeira C H, Alley M M, Jones B P. 2011. Evaluation of potentially labile soil organic carbon and nitrogen fractionation procedures. *Soil Biology & Biochemistry*, **43**, 438–444.

Tiessen H J W B, Stewart J W B, Cole C V. 1984. Pathways of phosphorus transformations in soils of differing pedogenesis. *Soil Science Society of America Journal*, **48**, 853–858.

Wan S Z, Lin G G, Liu B, Ding Y D, Li S L, Mao R. 2022. Contrasting responses of soil phosphorus pool and bioavailability to alder expansion in a boreal peatland, Northeast China. *Catena*, **212**, 106128.

Wang C W, Xie Y K, Tan Z X. 2024. Soil potassium depletion in global cereal croplands and its implications. *Science of the Total Environment*, **907**, 167875.

Wang H Y, Zhou J M, Du C W, Chen X Q. 2010. Potassium fractions in soils as affected by monocalcium phosphate, ammonium sulfate, and potassium chloride application. *Pedosphere*, **20**, 368–377.

Wang M J, Feng X Q, Zhou Z Y, Ma H Y, Ge T D, Tang C X, Wang D Y, Chen S. 2024. Labile organic carbon fractions in the rhizosphere contribute to nitrogen and phosphorus uptake in rice under long-term crop rotations and nitrogen application. *Applied Soil Ecology*, **200**, 105459.

Wang M M, Zhang S, Wang G C, Xiao L J, Gu B J, Zheng M H, Niu S L, Yang Y H, Luo Y Q, Zhang G L, Shi Z, Luo Z K. 2025. Increased plant productivity exacerbates subsoil carbon losses under warming via nitrogen mining. *Nature Geoscience*, **18**, 510–517.

Wang X, Sheng L X, Li Y, Jiang H B, Lv Z Y, Qi W, Luo W B. 2022. Soil labile organic carbon indicating seasonal dynamics of soil organic carbon in northeast peatland. *Ecological Indicators*, **138**, 108847.

Wen J L, Li Z Y, Yao J F, Wang S, Liu Y, Liu Y. 2024. The combined application of organic and inorganic fertilizers improved the quality of colored wheat by physicochemical properties and rheological characteristics of starch. *International Journal of Biological Macromolecules*, **282**, 137175.

Wu H Q, Du S Y, Zhang Y L, An J, Zou H T, Zhang Y L, Yu N. 2019. Effects of irrigation and nitrogen fertilization on greenhouse soil organic nitrogen fractions and soil-soluble nitrogen pools. *Agricultural Water Management*, **216**, 415–424.

Wu Y, Zhao D Y, Wang Y H, Wang J P, Wu Y Y, Peng P H, Yang L Y, Wu Y H, Bing H J, Bol R. 2024. Plant species modulate wildfire effects on soil phosphorus fractions in alpine forest of Eastern Tibetan Plateau. *Forest Ecology and Management*, **573**, 122338.

Xia H, Wang J Y, Riaz M, Babar S, Li Y X, Wang X L, Xia X Y, Liu B, Jiang C C. 2024. Co-application of biochar and potassium fertilizer improves soil potassium availability and microbial utilization of organic carbon: A four-year study. *Journal of Cleaner Production*, **469**, 143211.

Xue H P, Zhou X, Chen Y Y, Tu L Y, Liu X Q, Jiang S W, Ji M, Leng C R, Shen Y A. 2025. Effects of historical dust-mediated atmospheric phosphorus deposition on phosphorus fractions in sediments and primary productivity of Dalongwan Maar Lake, Northeast China. *Palaeogeography, Palaeoclimatology, Palaeoecology*, **660**, 112679.

Yang C D, Zhang S H, Tan G Y, Zhu S Q, Wang J. 2024. Effects of cover crops and nitrogen fertilization on soil physical properties, carbon and nitrogen fractions, and winter wheat yield in the Chinese Loess Plateau: A 4-year field experiment. *Field Crops Research*, **312**, 109400.

Yang H K, Xiao Y, Zhang X, Huang X L, Fan G Q. 2022. Maize straw mulching with uniconazole application increases the tillering capacity and grain yield of dryland winter wheat (*Triticum aestivum* L.). *Field Crops Research*, **284**, 108573.

Yang W J, Yu J, Li Y H, Jia B L, Jiang L G, Yuan A J, Ma Y, Huang M, Cao H B, Liu J S, Qiu W H, Wang Z H. 2024. Optimized NPK fertilizer recommendations based on topsoil available nutrient criteria for wheat in drylands of China. *Journal of Integrative Agriculture*, **23**, 2421–2433.

Yuan S, Li R N, Zhang Y J, Luan H A, Tang J W, Wang L Y, Ji H J, Huang S W. 2024. Effects of long-term partial substitution of inorganic fertilizer with pig manure and/or straw on nitrogen fractions and microbiological properties in greenhouse vegetable soils. *Journal of Integrative Agriculture*, **23**, 2083–2098.

Yuan Z X, Guan Q W, Chen X L, Zou P J, Gu Y Q, Wu Q, Niu Y Y, Meshack A O. 2023. Tree diversity increases soil C and N stocks of secondary forests in subtropical China. *Catena*, **222**, 106812.

Zeng W J, Wang Z D, Chen X Y, Yao X D, Ma Z Q, Wang W. 2023. Nitrogen deficiency accelerates soil organic carbon decomposition in temperate degraded grasslands, *Science of the Total Environment*, **881**, 163424.

Zhai L C, Wang Z B, Zhai Y C, Zhang L H, Zheng M J, Yao H P, Lv L H, Shen H P, Zhang J T, Yao Y R, Jia X L. 2022. Partial substitution of chemical fertilizer by organic fertilizer benefits grain yield, water use efficiency, and economic return of summer maize. *Soil & Tillage*

Research, **217**, 105287.
Zhang F, Chen M R, Xing Y Y, Han J, Wang X K. 2025. Reduction of nitrogen fertilizer and simultaneously application of organic fertilizer optimizes yield, water productivity and nitrogen metabolism of spring maize by improving soil properties in the Loess Plateau of China. *Journal of Agriculture and Food Research*, **19**, 101634.
Zhang L H, Li J H, Chen S, Huang W L, Huang L L, Zhu H F, Tang Y X, Li H, You C M, Wang L X, Liu S N, Xu H W, Xu L, Tan B, Xu Z F, Zhu P, Yuan Y L, Yin R, Zhu Y W, Zhang L. 2025. Dynamics of soil phosphorus fractions during the early recovery stage of two typical plantations in China after strip clearcutting. *Catena*, **250**, 108767.
Zhang M Y, Riaz M, Liu B, Xia H, El-desouki Z, Jiang C C. 2020. Two-year study of biochar: Achieving excellent capability of potassium supply via alter clay mineral composition and potassium-dissolving bacteria activity. *Science of the Total Environment*, **717**, 137286.
Zhang Y Z, Resch M C, Schütz M, Liao Z Y, Frey B, Risch A C. 2024. Strengthened plant-microorganism interaction after topsoil removal cause more deterministic microbial assembly processes and increased soil nitrogen mineralization. *Science of the Total Environment*, **950**, 175031.
Zhang Z G, Wang J, Huang W B, Chen J L, Wu F Q, Jia Y Y, Han Y C, Wang G P, Feng L, Li X F, Lei Y P, Yang B F, Xiong S W, Xin M H, Li Y B, Wang Z B. 2022. Cover crops and N fertilization affect soil ammonia volatilization and N_2O emission by regulating the soil labile carbon and nitrogen fractions. *Agriculture*, *Ecosystems and Environment*, **340**, 108188.
Zhang Z T, Luo R Y, Liu Q H, Qiang W, Liang J, Hou E Q, Zhao C Z, Pang X Y. 2023. Linking soil phosphorus fractions to abiotic factors and the microbial community during subalpine secondary succession: Implications for soil phosphorus availability. *Catena*, **233**, 107501.
Zhao J, Ren T, Fang Y T, Zhang S T, Cong R H, Li X K, Lu Z F, Zhu J, Lu J W. 2025. Soil organic nitrogen sequestrated more in oilseed rape-rice rotation than in wheat-rice rotation under different fertilizations. *Agriculture*, *Ecosystems and Environment*, **381**, 109445.
Zhao S C, He P, Qiu S J, Jia L L, Liu M C, Jin J Y, Johnston A M. 2014. Long-term effects of potassium fertilization and straw return on soil potassium levels and crop yields in north-central China. *Field Crops Research*, **169**, 116–122.
Zhao Y N, Mao X X, Zhang M S, Yang W, Di H J, Ma L, Liu W J, Li B W. 2021. The application of Bacillus Megaterium alters soil microbial community composition, bioavailability of soil phosphorus and potassium, and cucumber growth in the plastic shed system of North China. *Agriculture*, *Ecosystems and Environment*, **307**, 107236.
Zhong Y Q W, Yan W M, Shangguan Z P. 2015. Soil carbon and nitrogen fractions in the soil profile and their response to long-term nitrogen fertilization in a wheat field. *Catena*, **135**, 38–46.
Zhou J Y, Gu B J, Schlesinger W H, Ju X T. 2016. Significant accumulation of nitrate in Chinese semi-humid croplands. *Scientific Reports*, **6**, 25088.
Zhu J, Li M, Whelan M. 2018. Phosphorus activators contribute to legacy phosphorus availability in agricultural soils: A review. *Science of the Total Environment*, **612**, 522–537.
Zuo H L, Xu W S, Liu Z Y, Smaill S J, Zhou X Q. 2023. Long-term plant diversity increases soil extractable organic carbon and nitrogen contents in a subtropical forest. *Science of the Total Environment*, **878**, 163118.

Executive Editor-in-Chief Jinshui Wu
Managing Editor Lujuan Sun